Chemical Engineering Journal 428 (2022) 131226

Contents lists available at ScienceDirect

Chemical Engineering Journal

journal homepage: www.elsevier.com/locate/cej

Hyperbranched flame retardant for epoxy resin modification: Simultaneously improved flame retardancy, toughness and strength as well as glass transition temperature

Na Teng [a,c], Jinyue Dai [a,b,1], Shuaipeng Wang [a,b], Jingyuan Hu [a,b], Xiaoqing Liu [a,b,*]

[a] Zhejiang Key Laboratory of Marine Materials and Protective Technologies, Ningbo Institute of Materials Technology and Engineering, Chinese Academy of Sciences, Ningbo, Zhejiang 315201, China
[b] Key Laboratory of Marine Materials and Related Technologies, Chinese Academy of Sciences, Ningbo, Zhejiang 315201, China
[c] University of Chinese Academy of Sciences, Beijing 100049 China

ARTICLE INFO

Keywords:
Hyperbranched flame retardant
Epoxy resin
Strength
Toughness
Glass transition temperature

ABSTRACT

Endowing epoxy resins with simultaneously improved flame retardancy, toughness and strength as well as glass transition temperature (T_g) is a big challenge for us. Herein, a hyperbranched flame retardant (HBFR) with rigid backbone structure was synthesized through a facile strategy. Upon the incorporation of HBFR, the modified diglycidyl ether of bisphenol A (DGEBA) with phosphorus content of only 0.24 wt% exhibited better flame retardancy beyond expectation, showing UL-94 V-0 rating and limited oxygen index (LOI) above 32.6 vol%. Meanwhile, the modified epoxy resin demonstrated superior toughness, indicated by the more than 96% increment in impact strength both at 25 and −196°C, due to the enlarged free volume originated from hyperbranched structures. Furthermore, the T_g, flexural strength and modulus of modified epoxy systems were also significantly increased because of the rigid backbone structure and high crosslinking density afforded by HBFR. This work provided us an attractive strategy for simultaneously improving the flame retardancy, toughness, T_g and strength of commercial epoxy resins.

1. Introduction

Epoxy resin, as one of the most important thermosetting resins, has been extensively used in coatings, adhesives, electronics and structural components due to their high chemical resistance coupled with good electrical insulation, thermal and mechanical properties.[1,2] However, the mostly used diglycidyl ether of bisphenol A (DGEBA), owning more than 90% market share, suffers from an inherent shortcoming of high flammability, which seriously limits its application fields, and how to efficiently improve its fire resistance is always an important subject.[3,4]

Traditionally, the incorporation of halogen-containing compounds was considered as an appealing method to endow epoxy resins with improved flame resistance, due to the low cost, high flame-retardant efficiency, and little negative effects on the thermal or mechanical properties of target products.[5] However, concerns about the persistence and accumulation of halogenated flame retardants, combined with the release of toxic and corrosive fumes during combustion, have already resulted in strict restrictions on their application fields.[6,7] Currently, phosphorus-containing compounds have been regarded as one of the most promising flame retardants because of their chemical versatility, safety and high flame retardancy.[8,9] Among them, 9, 10-dihydro-9-oxa-10-phosphaphenanthrene-10-oxide (DOPO) is a widely explored one.[10] In Wang's work, a novel flame-retardant epoxy resin with UL-94 V-0 rating was synthesized from DOPO and DGEBA via a straightforward method. However, the high phosphorus content of 2.23 wt% seriously compromised the T_g with 22.5% reduction of modified systems.[11] Therefore, the loading reduction of phosphorus received wide attention, and composite fire retardants were frequently reported.[12–15]

Besides intrinsic flammability, the cured epoxy resins also show high brittleness, and their toughness improvement is of great significance and

* Corresponding author at: Zhejiang Key Laboratory of Marine Materials and Protective Technologies, Ningbo Institute of Materials Technology and Engineering, Chinese Academy of Sciences, Ningbo, Zhejiang 315201, China.
E-mail address: liuxq@nimte.ac.cn (X. Liu).
[1] Equal contribution to the first author

https://doi.org/10.1016/j.cej.2021.131226
Received 5 April 2021; Received in revised form 3 June 2021; Accepted 6 July 2021
Available online 11 July 2021

highly desired.[16,17] As we know, a widely taken strategy to improve epoxy resin's toughness is the introduction of hyperbranched compounds which showed low viscosity and high solubility.[18–20] For instance, Yang once reported that the tensile and impact strength of DGEBA at 77 K could be greatly improved by the introduction of hydroxyl functionalized hyperbranched polymer.[21] Ma and his coworkers synthesized several 1,3,5-hexahydro-striazine-containing hyperbranched epoxy resins, which led to 190.4% increments in the impact strengths of DGEBA.[22] The flame retardant was also often introduced into hyperbranched polymers (HBPs) to give DGEBA improved toughness and flammability.[23,24] Zhang synthesized a bio-based hyperbranched flame retardant (HBFR) from itaconic anhydride. It significantly improved both the toughness and fire safety of DGEBA. However, the flexible aliphatic chain of synthesized HBFR led to a dramatically decreased T_g.[23] Certainly, the increased T_g could be achieved in the aliphatic HBFR containing systems. But their modulus and strength were usually depressed.[25] To overcome this dilemma, the stiff backbone was incorporated into HBFR, but the negative effects caused by additional internal defects in heterogeneous system on T_g cannot be overlooked.[26,27] Therefore, the balance between mechanical performance and T_g of hyperbranched structure containing epoxy system is an important and difficult problem. To the best of our knowledge, the synergistic effect of HBFR's chemical and topological structures was seldom noticed, and the HBFR can significantly improve the toughness and flame retardancy of epoxy resin, and simultaneously increase its T_g, modulus and strength, has rarely been reported.

In this work, a HBFR was synthesized from 1,3,5-triglycidyl isocyanurate and 6-(bis(4-hydroxy-3-methoxyphenyl)methyl)dibenzo [c, e] oxaphosphinine 6-oxid (BDB) (Fig. 1). The combination of phosphorus and nitrogen was taken to improve the fire safety of DGEBA at a low phosphorus content. The hyperbranched structure was tried to enhance the toughness. And the more exciting idea was that the rigid BDB was employed to increase the stiffness of synthesized HBFR, and the multiple epoxy groups in HBFR would endow the cured systems with increased crosslink density and good compatibility. Herein, the chemical and topological structures of flame retardant were regulated at the same time, and the objective is to provide us a feasible method to simultaneously improve the flame retardancy, toughness, T_g and strength of epoxy resins.

2. Experimental

2.1. Raw materials

Vanillin (98.0%), guaiacol (98.0%), *p*-toluenesulfonic acid monohydrate (p-TSA, 98.5%), tetrabutylammonium bromide (TBAB, 99.0%) and 4,4-diaminodiphenylmethane (DDM, 98.0%) were supplied by Aladdin Reagent, China. Sodium hydroxide (96.0%), chloroform (99.0%), and petroleum ether (98.0%) were acquired from Sinopharm Chemical Reagent Co., Ltd. 9, 10-dihydro-9-oxa-10-phosphaphenanthrene-10-oxide (DOPO, 98%) were obtained from Guizhou Yuanyi Mining Group Co., Ltd., China. 1,3,5-triglycidyl isocyanurate (TGIC) were supplied by Shanghai Titan Scientific CO., Ltd. Diglycidyl ether of bisphenol A (DER331, epoxy value of 0.51–0.53 mol/100 g) was purchased from Dow Chemical Company. All the chemicals were used as received without further purification.

2.2. Synthesis of HBFR

Firstly, BDB was synthesized from DOPO, vanillin and guaiacol following the protocol reported in previous literature.[28] Then 14.23 g (0.03 mol) BDB and 150 mL DMSO were mixed with 29.72 g (0.1 mol) TGIC in a 250 mL three-necked round bottom flask equipped with a magnetic stirrer and a reflux condenser. The mixture was heated at 130–140°C for 12 h. After that, the mixture was naturally cooled down to room temperature and then extracted with 300 mL of chloroform. The organic phase was washed with deionized water, dried over magnesium sulfate anhydrous, filtered, precipitated in petroleum ether and dried under reduced pressure to afford the desired products (light-yellow powder HBFR). The synthetic route and structure of HBFR is illustrated in Fig. 1.

2.3. Preparation of flame-retardant epoxy composites

HBFR modified epoxy composites were fabricated via the reaction between DGEBA, HBFR and stoichiometric curing agent (DDM). Firstly, various contents of HBFR were mixture with DGEBA and stirred at 140°C to obtain transparent and uniform liquid. After cooling to 120°C, a specific amount of DDM was dissolved into the liquid mixtures. Subsequently, the mixtures were vacuum degassed at 120°C for 3 min, and then poured into preheated molds. After being step-cured under programmed heating conditions (140°C × 2 h, 160°C × 2 h, 180°C × 2 h, and 200°C × 2 h), the cured epoxy resins were allowed to slowly cool to room temperature. The detailed formulas were shown in Table 1.

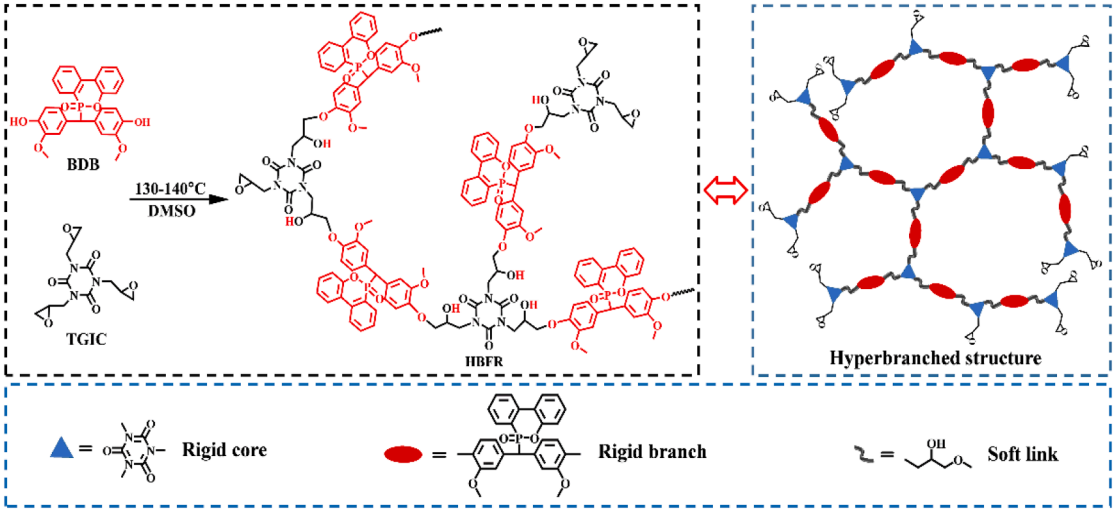

Fig. 1. Synthetic route and chemical structure of HBFR.

Table 1
Formulations and basic properties of different sample.

Samples	Composition (phr)			Content of P(wt%)	Gel time at 150°C	T_{d5} (°C)	Char yield at 800°C (%)	R_{max} (%/°C)
	DGEBA	HBFR	DDM					
EP	100	0	25.8	0	6.8	389	15.0	2.6
EP5	95	5	25.0	0.12	6.4	387	17.1	2.4
EP10	90	10	24.2	0.24	6.0	384	18.3	2.1
EP15	85	15	23.4	0.36	5.0	384	18.8	2.0

2.4. Measurements

Fourier transform infrared (FT-IR) analyses were carried out with a NICOLET 6700 spectrometer (Thermo-fisher, US) from 400 to 4000 cm^{-1}. ^{1}H, ^{13}C and ^{31}P nuclear magnetic resonance (NMR) spectra were collected on a 400 MHz AVANCE III Bruker NMR spectrometer (Bruker, Switzerland) with $CDCl_3$ or DMSO as solvent. The molecular weight and molecular weight distribution of HBFR were determined on a Waters 1515 gel permeation chromatography (GPC, Waters, US) instrument by using N,N-dimethylformamide as the eluent and linear polystyrene for calibration. The epoxy value of HBFR was obtained by hydrochloric acid-acetone titration method. The rheological behavior of resin mixture was investigated by a discovery hybrid rheometer (DHR-3) (TA, US) using plates with 20 mm diameter and 1 mm gap. To study the effect of temperature on viscosity, the sample was measured from 25 to 200°C at a heating rate of 3°C/min. The isothermal measurements were also carried out at different constant temperatures with a frequency and deformation amplitude of 10 rad/s and 1%, respectively. All samples were equilibrated at 25°C for 5 min before being transferred to the rheometer plate. The curing condition and curing behavior of epoxy thermosets were determined on a Mettler-Toledo MET DSC (METTLER TOLEDO, Switzerland) from 25 to 250°C at different heating rates of 5, 10, 15 and 20°C/min. DSC was also used to determine the T_g of cured resin, and the value was obtained from the second heating rate curve. All the differential scanning calorimetric (DSC) measurements were conducted under high purity nitrogen atmosphere with a flow rate of 20 mL/min. Thermogravimetric analyses (TGA) were performed using a Mettler-Toledo TGA/DSC1 (METTLER TOLEDO, Switzerland) under a nitrogen atmosphere with a heating rate of 20°C/min. The three-point bending tests were conducted on an Instron 5567 tester (Instron, US) with a rate of 5 and 2 mm/min, respectively. The notched impact strength was determined using a GT-7045-HML impact tester (GOTECH, China) with a 1.0 J pendulum at 25 and −196°C, respectively. Thermomechanical analyses (TMA) were performed on a TMA402 F3 tester (NETZSCH, Germany) with a heating rate of 3°C/min. Dynamic mechanical analyses (DMA) were carried out using a DMA Q800 instrument (TA, US). The tests were performed in tension mode with amplitude of 10 mm and at a frequency of 1 Hz. During measurements, the sample with dimension of 20 mm × 5 mm × 0.5 mm were heated from −110 to 250°C at a heating rate of 3°C/min. The UL-94 tests were conducted on a CZF-3 instrument (Jiangning Analysis Instrument Company, China) according to ASTM D3801. The LOI values were acquired according to ASTM D2863-97 using an HC-2 Oxygen Index instrument (Jiangning Analytical Instrument Co. Ltd., China). Cone calorimeter tests (CCT) were carried out on a 6810-cone calorimeter (Suzhou Yangyi Vouch Testing Technology Co. Ltd., China) according to GB/T 16172:2007. The fractured surfaces after impact tests were analyzed using scanning electron microscope (SEM, Regulus8230, Hitachi, Japan) equipped with energy dispersive spectroscopy (EDS, XFlash 6|100, Bruker, Switzerland). S4800 scanning electron microscope (Hitachi, Japan) was used to characterize the morphology of residual char after combustion. The phosphorus contents of HBFR were determined by using inductively coupled plasma/optical emission spectrometer (ICP-OES, Spectro ArcosII, Spectro, Germany).

3. Results and discussion

3.1. Synthesis of hyperbranched flame retardant (HBFR)

HBFR was synthesized by a typical $A_2 + B_3$ polymerization reaction. The A_2 monomer i.e., BDB, was synthesized by a single step reaction from DOPO, vanillin and guaiacol. The chemical structure of BDB was confirmed by FT-IR, ^{1}H, ^{13}C, and ^{31}P NMR spectra (Fig. S1), and the results exactly aligned with those in previous literature.[28] The FT-IR, ^{1}H, and ^{31}P NMR spectra of synthesized HBFR were displayed in Fig. S2. The characteristic peaks showing at 1143, 1207 and 1594 cm^{-1} were assigned to P-O-C_{Ar}, P = O and P-C_{Ar} stretching vibrations, confirming the presence of phosphaphenanthrene groups in the compound.[29] In addition, the presence of oxirane groups in HBFR was indicated by the absorption band observed at 858, 918, 1029, 1236 cm^{-1}.[30] Meanwhile, the characteristic signals for epoxy groups could also be observed at 2.59, 2.78 ppm (C***H***$_2$ of epoxy group), and 3.04–3.52 ppm (C***H*** of epoxy group)] in ^{1}H NMR. In addition, only one resonance peak appeared at 33.02 ppm in ^{31}P NMR, indicating that BDB does not exist in the target product. All these results indicated the successful synthesis of HBFR. The number-average molecular weight and molecular weight distribution of HBFR measured by GPC were found to be 3472 and 1.8, respectively. The epoxy value of HBFR was 0.20 mol/100 g determined by standard titration method.

3.2. Processability of DGEBA/HBFR/DDM mixtures

The processability of DGEBA/HBFR/DDM blends is strongly dependent on their rheological properties, and viscosity is one of the most important rheological parameters for flow properties description. Therefore, the temperature dependence of viscosity as well as time dependence of viscosity at certain temperature are extensively investigated. As expected, HBFR modified DGEBA exhibited much lower viscosity than those systems containing thermoplastic tougheners, due to lack of intermolecular entanglement in HBFRs. Specifically, as shown in Table 1 and Fig. 2a, the viscosity of EP15 at 40°C was lower than 0.5 Pa·s. In contrast, DGEBA modified by the thermoplastic modifiers, such as polyetherimide (PEI) and polyether sulphone (PES), showed much higher viscosities above 10 Pa·s at the same temperature and tougheners content.[31,32] Additionally, it was observed that the viscosity of DGEBA/HBFR/DDM mixture decreased with the increasing loading of HBFR, and all the mixed systems demonstrated stable viscosity lower than 1 Pa·s, when the temperature increased from 40 to 130°C. And after the temperature exceeded 135°C, as expected, the viscosity of all the systems increased quickly. The inserted image in Fig. 2a visually illustrated the satisfied low viscosity of EP15 system at 25°C. It is widely recognized that the liquid epoxy resins, which are suitable for resin transfer molding (RTM) process, should have low viscosity below 1 Pa·s and this viscosity value could maintain for a sufficient time (usually more than half an hour) at the processing temperature.[33,34] Fig. 2b shows the time dependence of viscosity at varied temperatures of 90, 100, and 110°C for EP15 system. As noticed, it kept its viscosity below 1 Pa·s at 90°C for 41 min, at 100°C for 24 min and at 110°C for 18 min, which indicated its suitability for RTM process. For comparison, the viscosity change of pristine DGEBA with time at different temperatures was illustrated in Fig. 2c. At the same temperature, pristine DGEBA

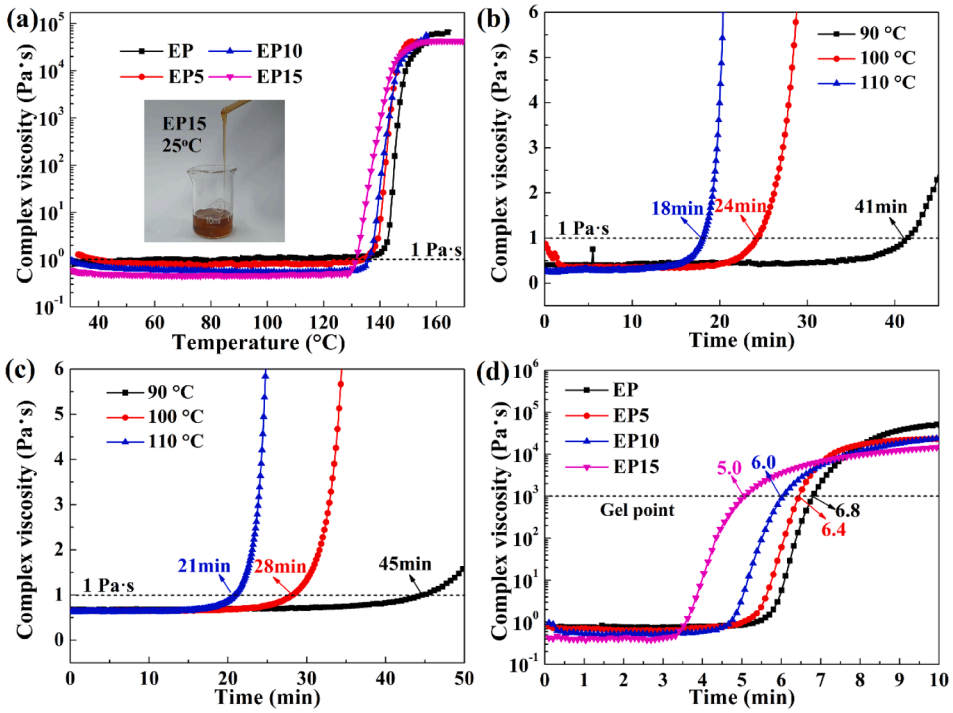

Fig. 2. Viscosity as a function of temperature with the heating rate of 3°C/min for all systems (a), viscosity *vs.* time curves at different temperatures for EP15 (b) and EP (c), viscosity *vs.* time curves for all systems at the temperature of 150°C (d).

showed a little more stable viscosity compared with those of EP15 system, indicating by the longer time for viscosity maintained below 1 Pa·s (45 min at 90°C, 28 min at 100°C, 21 min at 110°C), and the reason might be attributed to the improved curing activity of DGEBA/HBFR/DDM systems, catalyzed by the HBFR. In Fig. 2d, the gel time at 150°C for all the mixtures were compared. With the addition of HBFR, the gel time was decreased from 6.8 min for EP to 5.0 min for EP15, and this was line with the results from Fig. 2b and 2c. Usually, the steric hindrance of hyperbranched compounds will reduce the mobility of epoxy groups and some of them will be buried, which will decrease the accessibility of reactive epoxy groups to curing agent, and results in the impeded curing reactions.[35] In this work, the shorter gel time for DGEBA/HBFR/DDM systems was attributed to the presence of a large number of hydroxyl groups and tertiary amine, which could catalyze the epoxy-amine curing reaction.[36]

To further evaluate the catalyzing effect of HBFR on the curing reaction of DGEBA, the non-isothermal curing processes of different mixture systems at the heating rates of 5, 10, 15 and 20°C/min were traced. As displayed in Fig. S4a–d, the modified systems with varied HBFR loading exhibited lower exothermic peak temperature (T_p) than that for pristine DGEBA, suggesting their higher curing reactivity. Besides, the apparent activation energy (E_a) of them were calculated according to the following well-known Kissinger's (equation (1)) and the modified Ozawa's (equation (2)) equations.[37,38]

$$-\ln\left(\beta/T_p^2\right) = E_a/\mathrm{R}T_p - \ln(AR/E_a) \quad (1)$$

$$\ln\beta = -1.052 \times E_a/RT_p + \mathrm{C} \quad (2)$$

Where C is a constant, and β, T_p, E_a, R and A are the heating rate, absolute exothermic peak temperature, curing activation energy, ideal gas constant and pre-exponential factor, respectively. According to above equations, the plots of ln (β/T_p^2) and ln β versus $1/T_p$ should be straight lines, and E_a could be determined from the slope. As presented in Fig. S4e and f, both Kissinger's and Ozawa's methods were indicative of a decline in the value of E_a with the incremental content of HBFR, indicating increased reactivity towards heat curing reaction, which was in line with the decline of gel time.

3.3. Thermal stability

The thermal stability of epoxy composites under nitrogen atmosphere were assessed by TGA. As displayed in Fig. S5, the pristine epoxy resin underwent a one-step degradation process occurring approximately from 320 to 550°C, which was attributed to the thermal degradation of molecular chains through chain-scission and dehydration reactions.[39] In contrast, the epoxy composites containing HBFR exhibited the similar degradation process. However, the initial decomposition temperature and T_{d5} (the temperature of 5% mass loss) of them were tiny declined, indicating that HBFR led to the earlier decomposition. Those results could be explained by the lower thermal stability of P-C and O = P-O bonds in HBFR, compared with the C–C bond.[40] The degradation of DOPO groups produced phosphoric and polyphosphoric acid, which could accelerate the dehydration of epoxy resins and thus promoted charring behavior of epoxy resin proved by the char yield shown in Fig. S5 and Table 1. In addition, with the increasing content of HBFR, the maximum decomposition rate (R_{max}) of epoxy composites decreased from 2.6 %/°C for EP to 2.0 %/°C for EP15, which combined with the high char yield, might indicate the improved flame safety of DGEBA after the HBFR incorporation.

3.4. Thermal and mechanical properties

Due to the presence of multiple cavities in hyperbranched structure, HBPs-containing thermosets usually possess enhanced segment mobility and reduced T_g.[41] In order to avoid or limit these negative effects, the rigid compounds, 1,3,5-triglycidyl isocyanurate and BDB, were taken to construct the hyperbranched structure in this work. Thus, it was expected that the synthesized HBFR could confer epoxy composites with constant or even improved T_g. Fig. 3a–c and Table 2 indicate the T_g of epoxy composites with varied content of HBFR, which was determined by DSC and DMA (defined as the peak (α-relaxation) temperature in the dissipation factor (tan δ) *vs* temperature curve, in Fig. 3c). Although the

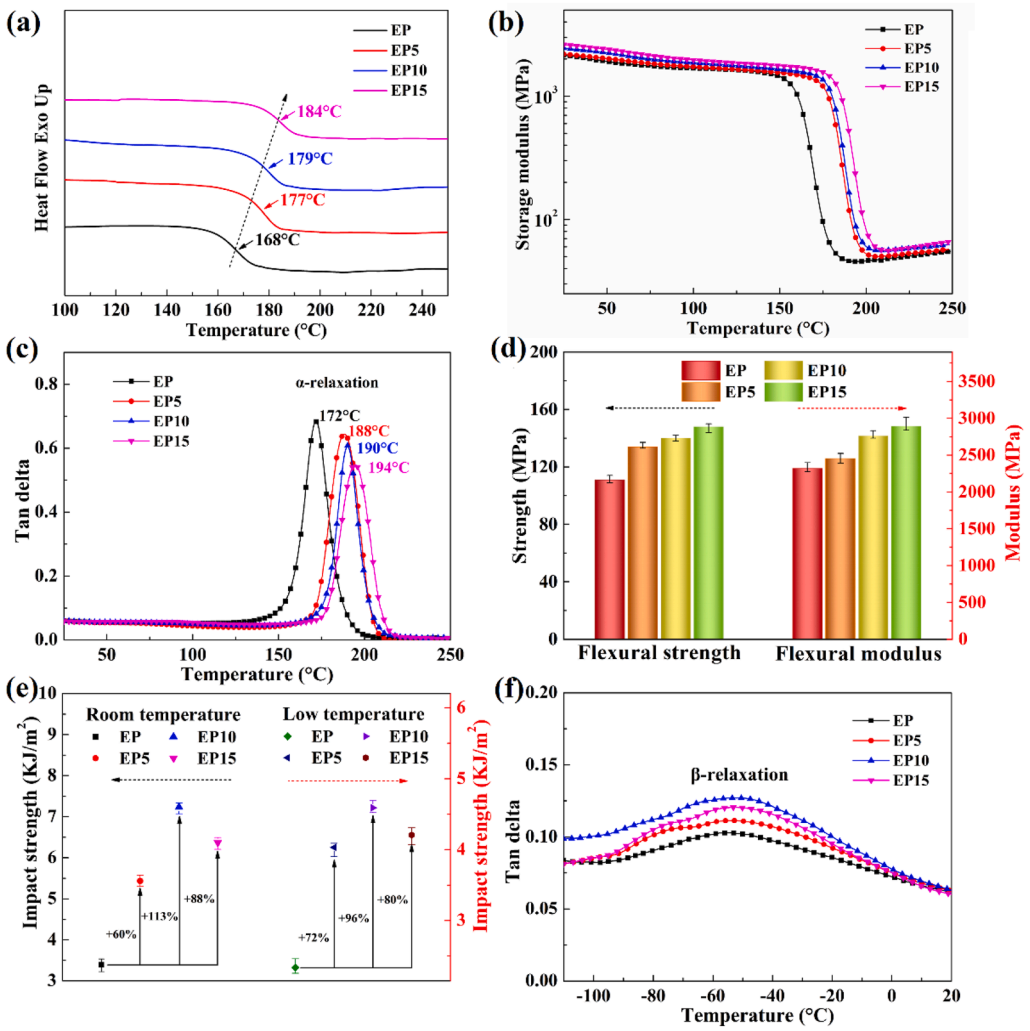

Fig. 3. DSC curves at different loading (a), variation of storage modulus (b) and tan δ (c, f) with temperature, effects of HBFR loading on flexural properties (d) and impact strength (e) for epoxy thermosets.

Table 2
T_g and physical parameters of epoxy thermosets.

Samples	T_g based on DSC (°C)	T_g based on DMA (°C)	$V_e^{'}$ ($\times 10^3$ mol·m^{-3})	$\alpha_{v,g}$ ($\times 10^{-6}$ K^{-1})	$\alpha_{v,r}$ ($\times 10^{-6}$ K^{-1})	$\Delta\alpha_v$ ($\times 10^{-6}$ K^{-1})
EP	168	172	4.03	63.9	166.0	102.1
EP5	177	188	4.33	60.9	175.0	114.1
EP10	179	190	4.76	60.3	176.5	116.2
EP15	184	194	5.01	59.8	176.8	117.0

variation of specific value is inevitable when different methods (DSC and DMA) are taken to measure the T_g, the trend of obtained results should be consistent. As expected, the T_g of HBFR containing systems were all higher than that of pristine DGEBA system. Besides, the values of T_g were found to steadily increase with the increasing content of HBFR, from 168°C for EP to 184°C for EP15 determined by DSC (Fig. 3a), and they were from 172 to 194°C measured by DMA (Fig. 3c). The improvement in T_g was most probably associated with the rigid structures and higher crosslink density of epoxy composites after the addition of HBFR. The cross-linking density was calculated by the following equation,[42,43] and related values were listed in Table 2:

$$V_e^{'} = E^{'}/3RT \quad (3)$$

Where E' is the storage modulus in the rubbery plateau region shown in Fig. 3b, R is the universal gas constant and T is the absolute temperature. In this work, the absolute temperature of $T_g + 50$ K was selected for the calculation of $V_e^{'}$. As expected, the cross-linking density of epoxy composites was steadily increased with the increasing content of HBFR, which provided a good explanation for the improved T_g.

It is widely accepted that the high cross-linking density and plenty of rigid groups are the key factors to improve the modules or stiffness of thermosets. As could be seen from Fig. S6 and Fig. 3d, the flexural modulus of epoxy composites was gradually increased with the increasing HBFR content. The highest flexural modulus of 2890 MPa was observed for EP15, which was 24.6% higher than that of EP (2320 MPa). With regard to the flexural strength, it was also showing an increasing trend from 111 MPa for EP to 148 MPa for EP15. As shown in Fig. 3e, with the introduction of HBFR, the impact strength of epoxy composites firstly increased and then decreased. At room temperature, when the content of HBFR reached 10 wt%, the maximum impact strength value of 7.2 KJ/m^2 was obtained for EP10, which was 113% higher than that of EP (3.4 KJ/m^2). After the specimens were quenched in liquid nitrogen, the impact strength was decreased to 2.3 KJ/m^2 for EP, and EP10 also demonstrated the highest value of 4.6 KJ/m^2. As we know, the free volume afforded by the intramolecular cavities in HBFR will lead to the increased impact strength. And in this work, as above demonstrated, the crosslinking density and rigidity of epoxy composites were also

increased with the introduction of HBFR, which was not conducive to improve the toughness. Therefore, it was not surprising to find that the impact strength showed an apparent reduction when the content of HBFR exceeded 10 wt%. Nonetheless, the impact strength of EP15 still remained at a relatively high level (6.4 KJ/m^2 at 25°C and 4.2 KJ/m^2 at −196°C). The area of β-relaxation peak in DMA curve (tan δ *vs* temperature curve) is often taken to evaluate the toughness of polymers. The larger the β-relaxation peak area, the higher the toughness.[44] As shown in Fig. 3f, all the specimens exhibited obvious β-relaxation peak in the temperature range of −100 to 0°C, and from EP to EP15, the area for the peak firstly increased and then decreased with the increasing content of HBFR, which was highly consistent with the notched impact test results showing in Fig. 3e.

The toughness of EP to EP15 was further qualitatively characterized by the fractured surface SEM micrographs. As shown in Fig. S7, EP showed a very smooth appearance without any filaments. Whereas, the HBFR-containing specimens, from EP5 to EP15, displayed an increasing rougher morphology with many filaments (as marked by red arrows) and wrinkles, which was conducive to energy dissipation and then improve the toughness. According to the element distribution maps in Fig. S7, the C, O, N and P atoms were evenly dispersed in the cured systems, indicating a homogeneous structure without any phase separation between HBFR and DGEBA matrix. Therefore, the simultaneous improved strength and toughness could be well explained by the *in situ* homogeneous reinforcing and toughening mechanism.[18]

As discussed above, it was the intramolecular cavity in HBFR that endowed EP5 to EP15 with excellent toughness. This is mainly originated from the fact that the free volumes in polymers not only provides spaces for molecular chain movements, but also absorbs the extra impact energy.[45] Therefore, besides above qualitative characterization, it was necessary for us to investigate the quantitative change of free volumes in epoxy composites after the addition of HBFR. According to the free volume theory, the fractional free volume (f_T) can be expressed as follows:

$$f_T = f_g + \Delta\alpha_v(T - T_g) \tag{4}$$

$$\Delta\alpha_v = \alpha_{v,r} - \alpha_{v,g} \tag{5}$$

Where f_g is the fractional free volume at T_g, $\alpha_{v,r}$ is the Coefficient of Thermal Expansion (CTE) in hyperelastic state, $\alpha_{v,g}$ is the CTE in glassy state. From above equations, it was not difficult to note that there was a positive correlation between free volume and $\Delta\alpha_v$. Generally, epoxy thermosets are considered as isotropic materials, so the value of CTE is three times the linear coefficient value.[41] Herein, the Linear Coefficient of Thermal Expansion (LCTE) was determined by TMA, and the results were summarized in Table 2. As shown, the $\Delta\alpha_v$ values of EP to EP15 showed a monotonic increment with the increasing of HBFR content. And the value for EP10 was 14.0 % higher than that of EP. Therefore, the increment of fractional free volume caused by the introduction of HBFR could be confirmed, which was the reason for the superior toughness of epoxy composites.

3.5. Flame-retardant performance

To investigate the effect of HBFR on flame-retardant behaviors of epoxy composites, LOI and UL-94 vertical-burning tests for EP to EP15 were performed, and the detailed results were listed in Table 3. As expected, EP was highly flammable with the low LOI of only 23.5 vol% and showed no rating in UL-94 test. In a sharp comparison, with the addition of HBFR, the epoxy composites showed much higher flame retardancy without melt dripping. Specifically, the LOI increased up to 30.1 vol%, 32.6 vol% and 33.4 vol% for EP5, EP10 and EP15, respectively. Meanwhile, the EP10 (phosphorus content as little as 0.24 wt%) and EP15 (phosphorus content of 0.36 wt%) were rated to V-0 grade. In parallel, their digital photographs during UL-94 tests were displayed in Fig. 4. It

Table 3
UL-94 burning and LOI results of epoxy thermosets.

Samples	LOI value (vol%)	Vertical buring test			
		After-flame time		Dripping	UL-94 rating
		t_1 (s)	t_2 (s)		
EP	23.6	74.6	–	Yes	No rating
EP5	30.1	5.2	10.8	No	V-1
EP10	32.6	3.9	3.3	No	V-0
EP15	33.4	2.4	3.1	No	V-0

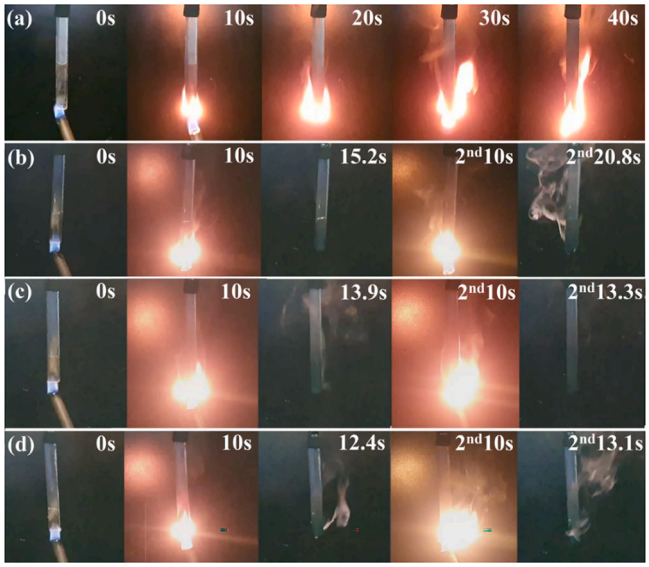

Fig. 4. Digital photographs of EP (a), EP5 (b), EP10 (c), and EP15 (d) during the vertical burning test.

was clearly noticed that both EP10 and EP15 self-extinguished within 4 s after the fire source was removed, and they released only a small amount of smoke during the whole combustion process. All these results preliminarily implied that the incorporation of HBFR endowed the epoxy composites with superior flame resistance.

To practically analyze the combustion behaviors of epoxy composites in real fires, cone calorimeter tests were performed. The corresponding combustion parameters including time to ignition (TTI), heat release rate (HRR), peak heat release rate (PHRR), total heat release (THR), smoke production rate (SPR), total smoke production (TSP), average effective heat of combustion (av-EHC), and average carbon monoxide yield (av-COY) were presented in Fig. 5 and Table 4. As indicated, with the introduction of HBFR, the TTI of epoxy composites decreased from 88 s for EP to 70 s for EP15. That was ascribed to the lower thermal stability of HBFR than DGEBA, and the free radicals produced by the degradation of HBFR catalyze the pyrolysis of epoxy matrix, which was in agreement with above TGA results. HRR, in particular PHRR, is regarded as one of the most important parameters to evaluate the fire dangers. As shown, the PHRR significantly decreased from 1005 kW/m^2 for EP to 479 kW/m^2 for EP15. Similarly, the THR values also reduced with the increasing content of HBFR, from 89.9 MJ/m^2 for EP to 68.7 MJ/m^2 for EP15. In addition, HBFR could slow down the SPR, and the TSP of epoxy composites were lower than that for EP, illustrating that the presence of HBFR could efficiently suppress the smoke formation during burning, thus improving the fire safety of epoxy resin. The smoke suppression might be relevant with the highly efficient charring effect of HBFR, which not only hinders the diffusion of the produced flammable gases, but also isolates the materials inside from fire.[46] Due to av-EHC reflecting the combustion degree of volatiles in the gas phase, the reduction of av-EHC after introducing HBFR indicates

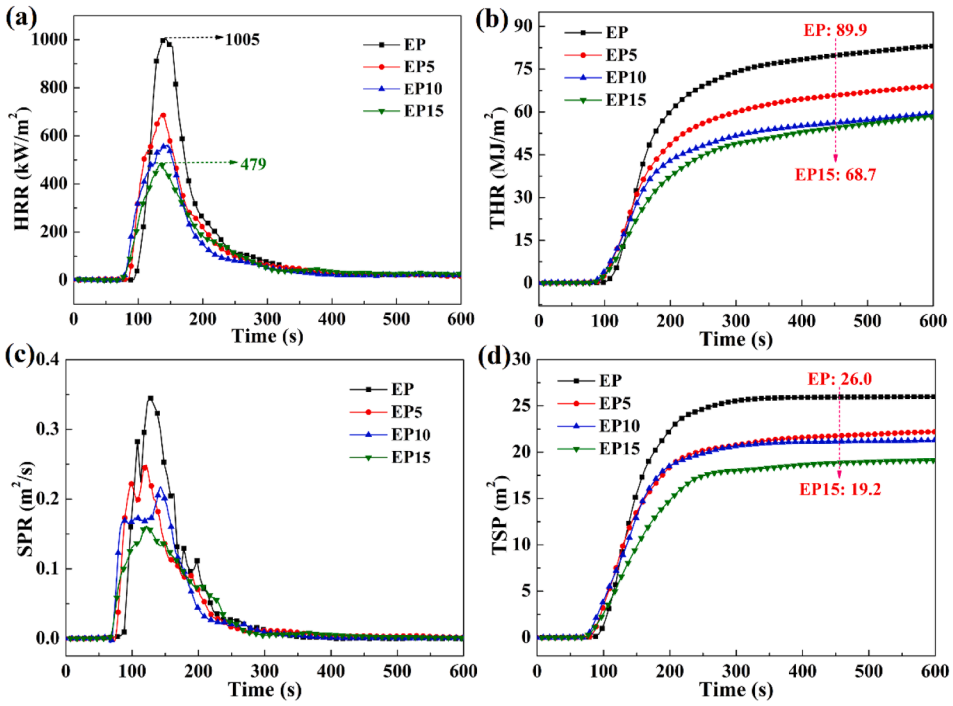

Fig. 5. HRR (a), THR (b), SPR (c), and TSR (d) curves of epoxy thermosets.

Table 4
Cone calorimeter tests results of epoxy thermosets.

Samples	TTI (s)	PHRR (kW/m^2)	THR (MJ/m^2)	av-EHC (MJ/kg)	av-COY (kg/kg)	TSP (m^2)
EP	88	1005	89.9	21.4	0.11	26.0
EP5	80	692	75.1	19.4	0.17	22.3
EP10	74	561	70.5	17.5	0.22	21.3
EP15	70	479	68.7	16.8	0.27	19.2

the presence of gaseous phase flame retardant effect in epoxy composites.[47] More carefully analyzing the combustion parameters, gaseous phase flame retardant mechanism could be further confirmed by the increase in the av-COY (resulting from insufficient combustion of volatiles).

Based on above results, it concluded that the addition of HBFR could not only significantly improve the toughness and flame retardancy of DGEBA, but also simultaneously increase its T_g, modulus and flexural strength. To compare with the literatures' values and perform a graphical evaluation, the toughness (impact strength), strength (flexural or

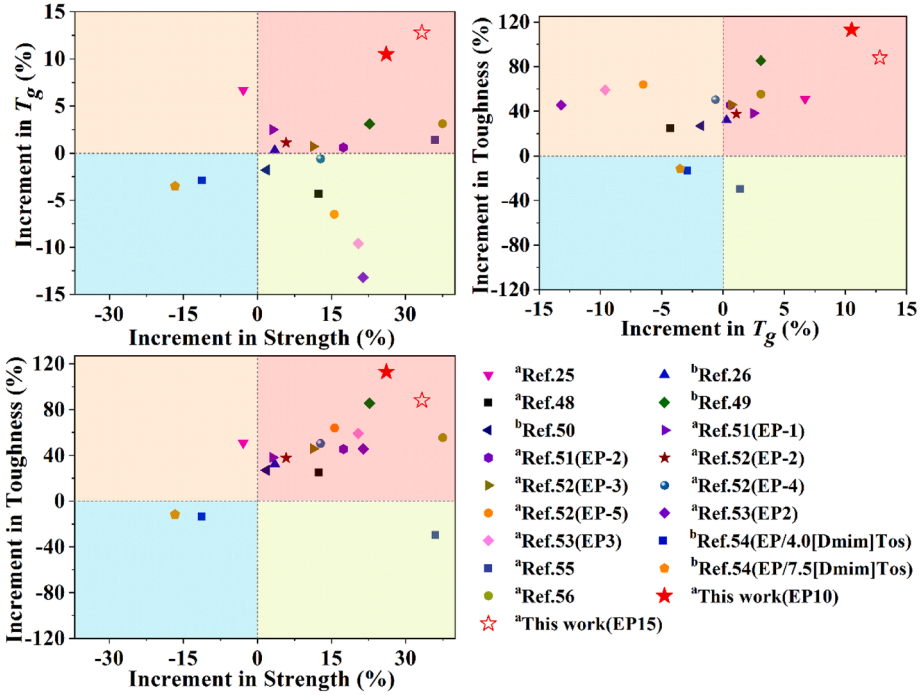

Fig. 6. Increments in toughness, strength (the superscript a is flexural strength, the superscript b is tensile strength), and T_g of previously reported UL-94 V-0 epoxy.

tensile strength), as well as the T_g of previously reported UL-94 V-0 epoxy resins were all presented in the 3D scatter plots (Fig. S8), [25,26,48–56] and for easy identification, the projections of these scatter dots onto the three coordinate planes were shown in Fig. 6. It was evident that only some points including those standing for EP10 and EP15 were always in the first quadrant of the three coordinate plans, which indicated simultaneously improved toughness, strength, and T_g compared to the pristine epoxy systems. Moreover, EP10 and EP15 demonstrated the largest increments in T_g, toughness, as well as strength, showing by the red five stars in Fig. 6.

3.6. Flame-retardant mechanism Analysis

3.6.1. Gaseous phase analysis

Fig. S9 displays the 3D spectra of gaseous phase during the thermal decomposition for EP and EP15, which provides qualitative information about the gaseous products. In general, EP presented higher gas releasing rate compared with EP15, suggesting its faster decomposition. In an attempt to deeply understand the mechanism, the FT-IR spectra of volatile pyrolysis products at maximum decomposition rates were presented in Fig. 7(a and b). Compared with EP, EP15 showed similar main degradation products indicating by the characteristic absorption bonds, which implied that the incorporation of HBFR did not change the degradation route of EP. For instance, the characteristic peaks showing at 3650 and 2974 cm^{-1} were assigned to H_2O and hydrocarbons compounds, respectively. The bands appearing at 1768 cm^{-1} were due to the stretching vibrations of C = O. The presence of aromatic compounds was indicated by the bands observed at 1607, 1507 and 829 cm^{-1}. Absorption bands showing at 1260 and 1176 cm^{-1} were representative of C-O containing compounds. Notably, besides aforementioned main degradation products, EP15 displayed the absorption bands for P-O at 1060 cm^{-1}, indicating that the phosphorus-containing chemicals played a fire-resistance role in gaseous phase. The absorption intensity of pyrolysis products for EP and EP15 *vs* time were illustrated in Fig. 7. The total pyrolysis products curves (Fig. 7(c)) clearly showed that EP15 released volatile products (at 28.2 min) earlier and simultaneously exhibited slower releasing rate than EP (at 29.8 min), which was due to the fact that HBFR catalyzed the thermal decomposition of DGEBA matrix and facilitated the formation of continuous carbon layer at relatively lower temperature accordingly. All these analyses coincided well with the TGA results. According to previous investigations on the thermal degradation mechanism of DGEBA, carbonyl compounds are mainly produced by the free-radical cracking reaction of hydroxyl-containing short fatty chains.[57] Interestingly, the release of carbonyl compounds was declined for EP15 when compared with EP (Fig. 7(d)), revealing the effective inhibition of free-radical cracking process in EP15 system. As a result, the dehydration reaction (proved by the release of H_2O in Fig. 7(h)) and cyclization reaction were promoted by HBFR, and residual char increased accordingly. Due to the relatively low thermal stability of C-N, the degradation of HBFR generated considerable N-containing non-flammable gases (N_2, NH_3, NO_2) and CO_2,[58] which could take away the heat as well as dilute the flammable gas and oxygen in the gas phase. In addition, HBFR not only facilitated the release of non-flammable gases such as H_2O, CO_2, but also restrained the release of flammable gases as revealed by the release of hydrocarbons, carbonyl, aromatic, and ethers compounds, et al., as revealed in Fig. 7.

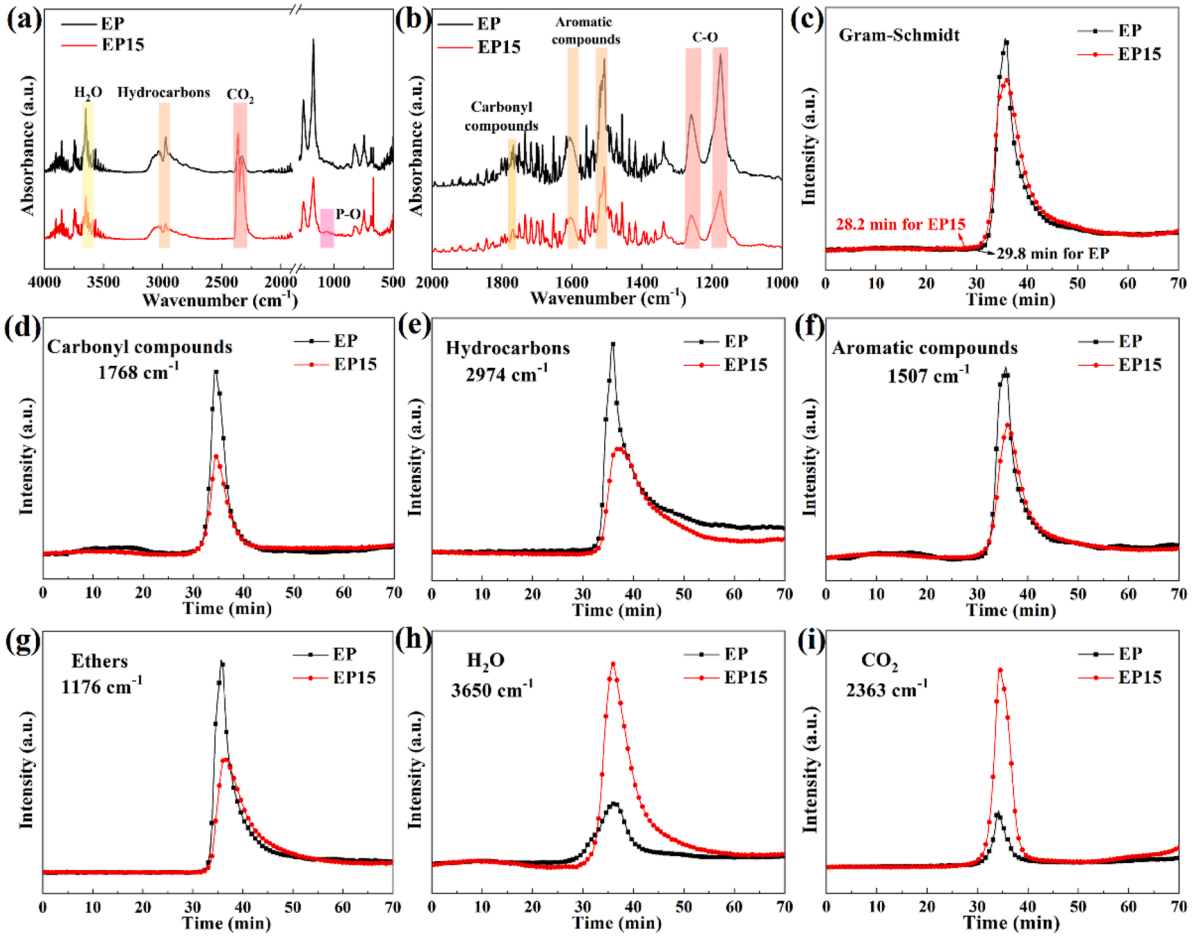

Fig. 7. FT-IR spectra of pyrolysis products for EP and EP15 at maximum decomposition rate (a) and (b); intensity of pyrolysis products (Total (c), Carbonyl compounds (d), Hydrocarbons (e), Aromatic compounds (f), Ethers (g), H_2O (h), CO_2 (i)) versus time for EP and EP15.

3.6.2. Condensed phase analysis

Normally, DOPO-containing flame retardants exert flame-retardant effects not only by releasing phosphorous-containing free radicals and non-flammable gases in the gaseous phase, but also by promoting the formation of compact swelling char layer with rich phosphorus in the condensed phase.[59] To further acquaint the flame-retardant mechanism, the condensed phases obtained after cone calorimeter tests were investigated. As depicted in Fig. 8(a), few of char residue was observed for EP, and the char residue was broken and discontinuous. This was probably ascribed to the rapid decomposition of DGEBA, which broke through the thin char layer. However, with the addition of HBFR, from EP5 to EP15, the char residue increased and gentler degradation happened, and thus the char layer became more and more compact, continuous and intumescent. Further analyzing the morphology of external and internal char residue by SEM (Fig. 8(b)), it was found that the external char residue of EP10 exhibited homogeneous and dense morphology, and the increasing content of HBFR made the external char residue be more compact and complete (from EP5 to EP15). As a result, the integrated char layer effectively prevented the transfer of heat, O_2 and flammable volatiles, revealing strong barrier effect. On the other hand, there were honeycomb-like hollow structures (indicated by red dotted circles) inside the compact char layer of epoxy composites, while fragmented internal residue char formed in EP during the combustion. In contrast to fragmented char layer, the honeycomb-like hollow structures were more conducive to reduce the heat transfer. Furthermore, the combination of compact external char layer and honeycomb-like hollow internal char residue was capable of storing considerable pyrolysis gases with masses of phosphorous free radicals and nonflammable gases during combustion, which were instantly released to snuff out the flame when the gas pressure in the interior was sufficient to break through the char layer.

To understand the formation process of above ingenious structures, the chemical composition of char residue was analyzed by FT-IR. As revealed in Fig. S10, an obvious absorption peak appeared at 1584 cm^{-1}, indicating that fused-ring aromatic compounds were formed in the carbon residue.[60] Moreover, an apparent band at 1068 cm^{-1}, which was attributed to the stretching vibrations of P-O-C_{Ar}, appeared in the carbon residue of EP15, while this peak was absent in the FT-IR spectra for EP. Therefore, it should be the phosphoric and polyphosphoric acid formed during the degradation of HBFR underwent esterification and dehydration reactions with the degraded epoxy matrix, forming the fused-ring aromatic compounds connected by P-O-C and enhancing the carbonaceous char,[61] which resulted in the dense char layer of epoxy composites.

Based on above analyses, the flame retardant mechanism for HBFR-containing systems was schematically illustrated as follows (Fig. 9). During the combustion, DOPO in HBFR pyrolyzed into PO·, PO_2· and polyphosphoric acid, which could not only suppress the chain radical reaction to decrease the release of flammable gases, but also catalyze dehydration and cyclization of epoxy matrix to form compact and continuous char layer in the condensed phase. The char layer protected the underlying polymeric substrate from heat and O_2, and prevented the release of ignitable gases simultaneously. Besides, the PO· and PO_2· quenched the active free radicals, and the massive nonflammable gases diluted the flammable gases, and consequently the combustion process was restrained in gaseous phase. In a word, the barrier effect of the compact and continuous char layers, the dilution effect of nonflammable gases, and the quenching effect of phosphorus-based free radicals synergistically improved the fire safety of the epoxy composites.

4. Conclusions

In this article, we demonstrated a facile approach to simultaneously endow epoxy resin (DGEBA) with excellent flame retardancy, increased toughness and strength, as well as elevated T_g, by incorporating a novel hyperbranched reactive flame retardant with rigid backbone structure (HBFR). A great many of intramolecular cavities in HBFR led to the remarkable increase of fractional free volumes of epoxy composites, which contributed significantly to the improvements in toughness by providing spaces for chain segments movement and absorbing extra energy. The impact strength of cure DGEBA was improved by 113% at 25°C and 96% at −196°C, when 10% HBFR was introduced (EP10). Moreover, due to the rigid backbone structure of HBFR and increased cross-linking density after curing reaction, the flexural strength,

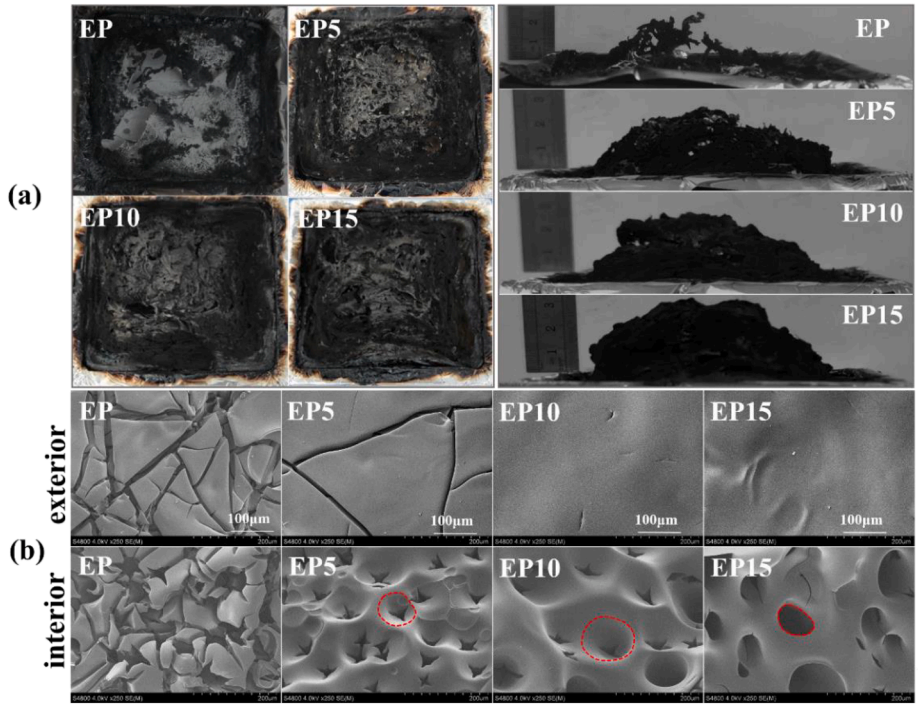

Fig. 8. Photographs of epoxy thermosets after cone calorimeter tests (a); SEM micrographs of char residue: external char residue and internal char residue (b).

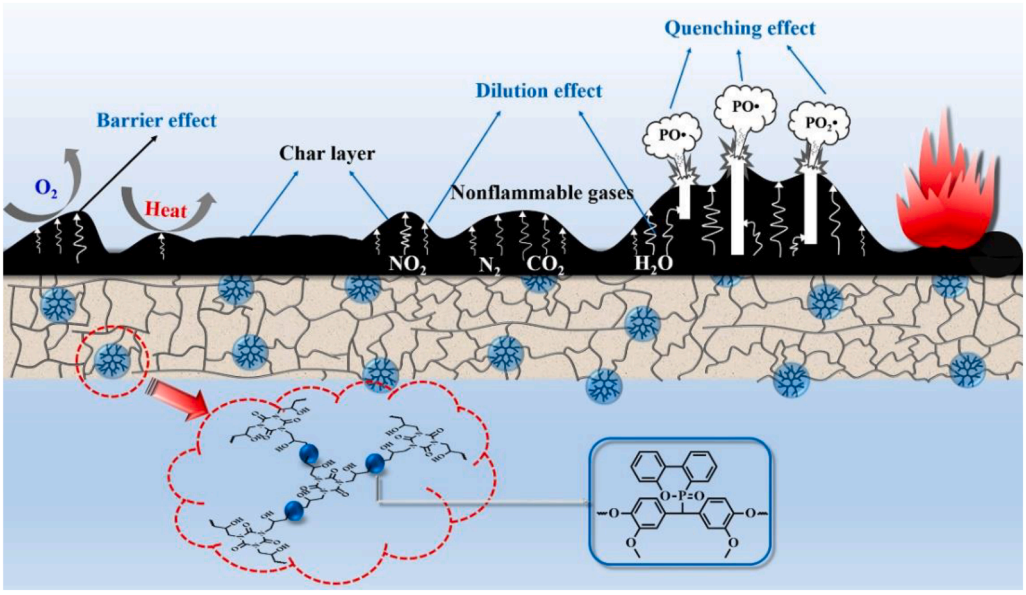

Fig. 9. The schematic diagram of the possible flame retardant mechanism of epoxy thermoset modified by HBFR.

modulus, and T_g of epoxy composites were all increased, from 111 MPa, 2320 MPa and 172°C for EP to 148 MPa, 2890 MPa and 194°C for EP15. In addition, the incorporation of HBFR promoted the formation of compact and continuous char layers, and facilitated the release of a large quantity of non-flammable gases as well as P·, PO· and PO_2·, which enabled epoxy composites to score UL-94 V-0 rating and high LOI (above 32.6 vol%) with content of phosphorus only 0.24 wt%. Based on this work, it concludes that simultaneously regulating the chemical and topological structures of hyperbranched flame retardant is a feasible approach to obtain the modified epoxy resins with improved flame retardancy, increased toughness and strength, as well as elevated T_g.

Declaration of Competing Interest

The authors declare that they have no known competing financial interests or personal relationships that could have appeared to influence the work reported in this paper.

Acknowledgments

The authors are grateful for the financial support from National Natural Science Foundation of China (Nos. U1909220 and 52003283), Zhejiang Provincial Natural Science Foundation of China (No. LR20E030001), Chinese Academy of Sciences (No. KFZD-SW-439), "Science and Technology Innovation 2025" Major Project of Ningbo (No. 2018B10013), National Ten Thousand Talent Program for Young Top-notch Talents, Ten Thousand Talent Program for Young Top-notch Talents of Zhejiang Province, Research Project of Technology Application for Public Welfare of Zhejiang Province (No. 202002N3122).

Appendix A. Supplementary data

Supplementary data to this article can be found online at https://doi.org/10.1016/j.cej.2021.131226.

References

[1] Q. Guo, Thermosets: structure, properties, and applications, Elsevier, 2018.
[2] M. Cui, S. Ren, H. Zhao, Q. Xue, L. Wang, Polydopamine coated graphene oxide for anticorrosive reinforcement of water-borne epoxy coating, Chem. Eng. J. 335 (2018) 255–266.
[3] F. Fang, S. Ran, Z. Fang, P. Song, H. Wang, Improved flame resistance and thermo-mechanical properties of epoxy resin nanocomposites from functionalized graphene oxide via self-assembly in water, Compos. Part B-Eng. 165 (2019) 406–416.
[4] J. Dai, N. Teng, J. Liu, J. Feng, J. Zhu, X. Liu, Synthesis of bio-based fire-resistant epoxy without addition of flame retardant elements, Compos. Part B-Eng. 179 (2019), 107523.
[5] A.D. La Rosa, A. Recca, J.T. Carter, P.T. McGrail, An oxygen index evaluation of flammability on modified epoxy/polyester systems, Polymer 40 (14) (1999) 4093–4098.
[6] S.L. Waaijers, D. Kong, H.S. Hendriks, C.A.D. Wit, I.T. Cousins, R.H.S. Westerink, P. E.G. Leonards, M.H.S. Kraak, W. Admiraal, P.D. Voogt, Persistence, bioaccumulation, and toxicity of halogen-free flame retardants, Rev. Environ. Contam. Toxicol. 222 (2013) 1–71.
[7] X. Zhou, S. Qiu, X. Mu, M. Zhou, W. Cai, L. Song, W. Xing, Y. Hu, Polyphosphazenes-based flame retardants: A review, Compos. Part B-Eng. 202 (2020) 108397, https://doi.org/10.1016/j.compositesb:2020.108397.
[8] F. Fang, P. Song, S. Ran, Z. Guo, H. Wang, Z. Fang, A Facile Way to Prepare Phosphorus-Nitrogen-Functionalized Graphene Oxide for Enhancing the Flame Retardancy of Epoxy Resin", Compos Commun 10 (2018) 97–102.
[9] S. Huo, P. Song, B. Yu, S. Ran, V.S. Chevali, L. Liu, Z. Fang, H. Wang, Phosphorus-containing flame retardant epoxy thermosets: Recent advances and future perspectives, Prog. Polym. Sci. 114 (2021) 101366, https://doi.org/10.1016/j.progpolymsci.2021.101366.
[10] S. Ran, F. Fang, Z. Guo, P. Song, Y. Cai, Z. Fang, H. Wang, Synthesis of decorated graphene with P, N-containing compounds and its flame retardancy and smoke suppression effects on polylactic acid, Compos Part B-Eng 170 (2019) 41–50.
[11] C.S. Wang, C.H. Lin, Synthesis and properties of phosphorus-containing epoxy resins by novel method, J. Polym. Sci. Part A-Polym. Chem. 37 (21) (1999) 3903–3909.
[12] S. Yang, J. Wang, S. Huo, L. Cheng, M. Wang, Preparation and flame retardancy of an intumescent flame-retardant epoxy resin system constructed by multiple flame-retardant compositions containing phosphorus and nitrogen heterocycle, Polym. Degrad. Stabil. 119 (2015) 251–259.
[13] Z. Zhang, D. Kong, H. Sun, L. Sun, C. Dong, Z. Lu, Synthetic novel, convenient and eco-friendly Si/P/N synergistic treatment agent to improve the flame retardancy and thermal stability of cotton fabrics, Cellulose 27 (17) (2020) 10473–10487.
[14] C. Bo, Z. Shi, L. Hu, Z. Pan, Y. Hu, X. Yang, P. Jia, X. Ren, M. Zhang, Y. Zhou, Cardanol derived P, Si and N based precursors to develop flame retardant phenolic foam, Sci. Rep. 10 (2020) 12082.
[15] F. Chu, C. Ma, T. Zhang, Z. Xu, L. Song, Renewable vanillin-based flame retardant toughening agent with ultra-low phosphorus loading for the fabrication of high-performance epoxy thermoset, Compos. Part B-Eng. 190 (2020), 107925.
[16] S.-Y. Fu, X.-Q. Feng, B. Lauke, Y.-W. Mai, Effects of particle size, particle/matrix interface adhesion and particle loading on mechanical properties of particulate–polymer composites, Compos. Part B-Eng. 39 (6) (2008) 933–961.
[17] F.H. Gojny, M.H.G. Wichmann, U. Kopke, Carbon nanotube-reinforced epoxy-composites: enhanced stiffness and fracture toughness at low nanotube content, Compos. Sci. Technol. 64 (2004) 2363–2371.
[18] S. Chen, Z. Xu, D. Zhang, Synthesis and application of epoxy-ended hyperbranched polymers, Chem. Eng. J. 343 (2018) 283–302.
[19] Z. Xu, Y. Liang, X.u. Ma, S. Chen, C. Yu, Y. Wang, D. Zhang, M. Miao, Recyclable thermoset hyperbranched polymers containing reversible hexahydro-s-triazine, Nat. Sustain. 3 (1) (2020) 29–34.
[20] X. Ma, W.Q. Guo, Z.J. Xu, S.F. Chen, J. Chen, J.H. Zhang, M.H. Miao, D.H. Zhang, Synthesis of degradable hyperbranched epoxy resins with high tensile, elongation,

modulus and low-temperature resistance, Compos. Part B-Eng. 192 (2020), 108005.
[21] J.P. Yang, Z.K. Chen, G. Yang, S.Y. Fu, L. Ye, Simultaneous improvements in the cryogenic tensile strength, ductility and impact strength of epoxy resins by a hyperbranched polymer, Polymer 49 (2008) 3168–3175.
[22] X. Ma, Y.Y. Liang, Z.Y. Xu, S.F. Chen, J. Cheng, M.H. Miao, D.H. Zhang, The versatility of hyperbranched epoxy resins containing hexahydro-s-triazine on diglycidyl ether of bisphenol-A composites, Compos. Part B-Eng. 196 (2020), 108109.
[23] J. Zhang, X. Mi, S. Chen, Z. Xu, J. Wang, A bio-based hyperbranched flame retardant for epoxy resins, Chem. Eng. J. 381 (2019), 122719.
[24] X. Li, Z. Zhao, Y. Wang, H. Yan, X. Zhang, B. Xu, Highly efficient flame retardant, flexible, and strong adhesive intumescent coating on polypropylene using hyperbranched polyamide, Chem. Eng. J. 324 (2017) 237–250.
[25] C. Ma, S. Qiu, B. Yu, J. Wang, C. Wang, W. Zeng, Y. Hu, Economical and environment-friendly synthesis of a novel hyperbranched poly (aminomethylphosphine oxide-amine) as co-curing agent for simultaneous improvement of fire safety, glass transition temperature and toughness of epoxy resins, Chem. Eng. J. 322 (2017) 618–631.
[26] C. Ma, S. Qiu, J. Wang, H. Sheng, Y.i. Zhang, W. Hu, Y. Hu, Facile synthesis of a novel hyperbranched poly(urethane-phosphine oxide) as an effective modifier for epoxy resin, Polym. Degrad. Stabil. 154 (2018) 157–169.
[27] J. Liu, S. Wang, Y. Peng, J. Zhu, W. Zhao, X. Liu, Advances in sustainable thermosetting resins: From renewable feedstock to high performance and recyclability, Prog. Polym. Sci. 113 (2021), 101353.
[28] J. Liu, J. Dai, S. Wang, Y. Peng, L. Cao, X. Liu, Facile synthesis of bio-based reactive flame retardant from vanillin and guaiacol for epoxy resin, Compos. Part B-Eng. 190 (2020), 107926.
[29] Y. Chen, H. Duan, S. Ji, H. Ma, Novel phosphorus/nitrogen/boron-containing carboxylic acid as co-curing agent for fire safety of epoxy resin with enhanced mechanical properties, J. Hazard. Mater. 402 (2021), 123769.
[30] X. Shen, X. Liu, J. Dai, Y. Liu, Y. Zhang, J. Zhu, How does the hydrogen bonding interaction influence the properties of furan-based epoxy resins, Ind. Eng. Chem. Res. 56 (38) (2017) 10929–10938.
[31] A. Bonnet, J.P. Pascault, H. Sautereau, Y. Camberlin, Epoxy diamine thermoset/thermoplastic blends. 2. Rheological behavior before and after phase separation, Macromolecules 32 (25) (1999) 8524–8530.
[32] K. Mimura, H. Ito, H. Fujioka, Improvement of thermal and mechanical properties by control of morphologies in PES-modified epoxy resins, Polymer 41 (12) (2000) 4451–4459.
[33] F.H. Gojny, M.H.G. Wichmann, B. Fiedler, W. Bauhofer, K. Schulte, Influence of nano-modification on the mechanical and electrical properties of conventional fibre-reinforced composites, Compos. Part A-Appl. Sci. Manuf. 36 (11) (2005) 1525–1535.
[34] J. Li, C. Zhang, R. Liang, B. Wang, Statistical characterization and robust design of RTM processes, Compos. Part A-Appl. Sci. Manuf. 36 (5) (2005) 564–580.
[35] R. Mezzenga, L. Boogh, J.-A. Månson, B.o. Pettersson, Effects of the branching architecture on the reactivity of epoxy-amine groups, Macromolecules 33 (12) (2000) 4373–4379.
[36] F. Ansari, S. Galland, M. Johansson, C.J.G. Plummer, L.A. Berglund, Cellulose nanofiber network for moisture stable, strong and ductile biocomposites and increased epoxy curing rate, Compos. Part A-Appl. Sci. Manuf. 63 (2014) 35–44.
[37] H.E. Kissinger, Reaction kinetics in differential thermal analysis, Anal. Chem. 29 (11) (1957) 1702–1706.
[38] T. Ozawa, A new method of analyzing thermogravimetric data, Bull. Chem. Soc. Jpn. 38 (11) (1965) 1881–1886.
[39] V. Bellenger, E. Fontaine, A. Fleishmann, J. Saporito, J. Verdu, Thermogravimetric study of amine cross-linked epoxies, Polym. Degrad. Stabil. 9 (4) (1984) 195–208.
[40] S. Qiu, Y. Zhou, X. Zhou, T. Zhang, C. Wang, R.K.K. Yuen, W. Hu, Y. Hu, Air-stable polyphosphazene-functionalized few-layer black phosphorene for flame retardancy of epoxy resins, Small (Weinheim an der Bergstrasse, Germany) 15 (10) (2019) 1805175, https://doi.org/10.1002/smll.v15.1010.1002/smll.201805175.
[41] T. Liu, Y. Nie, R. Chen, L. Zhang, Y. Meng, X. Li, Hyperbranched polyether as an all-purpose epoxy modifier: controlled synthesis and toughening mechanisms, J. Mater. Chem. A 3 (3) (2015) 1188–1198.
[42] J. Seo, N. Yui, J.-H. Seo, Development of a supramolecular accelerator simultaneously to increase the cross-linking density and ductility of an epoxy resin, Chem. Eng. J. 356 (2019) 303–311.
[43] S. Wang, N. Teng, J. Dai, J. Liu, L. Cao, W. Zhao, X. Liu, Taking advantages of intramolecular hydrogen bonding to prepare mechanically robust and catalyst-free vitrimer, Polymer 210 (2020), 123004.
[44] D. Zhang, D. Jia, Toughness and strength improvement of diglycidyl ether of bisphenol-A by low viscosity liquid hyperbranched epoxy resin, J. Appl. Polym. Sci. 101 (4) (2006) 2504–2511.
[45] C. Gao, D. Yan, Hyperbranched polymers: from synthesis to applications, Prog. Polym. Sci. 29 (2004) 183–275.
[46] Y. Feng, C. He, Y. Wen, Y. Ye, X. Zhou, X. Xie, Y.-W. Mai, Superior flame retardancy and smoke suppression of epoxy-based composites with phosphorus/nitrogen co-doped graphene, J. Hazard. Mater. 346 (2018) 140–151.
[47] J. Zhao, X.u. Dong, S. Huang, X. Tian, L. Song, Q. Yu, Z. Wang, Performance comparison of flame retardant epoxy resins modified by DPO-PHE and DOPO-PHE, Polym. Degrad. Stabil. 156 (2018) 89–99.
[48] X.F. Liu, B.W. Liu, X. Luo, D.-M. Guo, H.-Y. Zhong, L. Chen, Y.-Z. Wang, A novel phosphorus-containing semi-aromatic polyester toward flame retardancy and enhanced mechanical properties of epoxy resin, Chem. Eng. J. 380 (2020), 122471.
[49] Q.V. Bach, C.M. Vu, D.D. Nguyen, B.X. Kien, Impacts of phosphorous-linked epoxidized vegetable oil on mechanical behaviors and flammability properties of silica reinforced epoxy composite, Thermochim. Acta 691 (2020), 178722.
[50] M. Zhu, L. Liu, Z. Wang, Mesoporous silica via self-assembly of nano zinc amino-tris-(methylenephosphonate) exhibiting reduced fire hazards and improved impact toughness in epoxy resin, J. Hazard. Mater. 392 (2020), 122343.
[51] Z. Li, M. Chen, S. Li, X. Fan, C. Liu, Simultaneously improving the thermal, flame-retardant and mechanical properties of epoxy resins modified by a novel multi-element synergistic flame retardant, Macromol. Mater. Eng. 304 (2019) 1800619.
[52] S. Li, M. Chen, L. Su, X. Lin, C. Liu, Highly efficient multielement flame retardant for multifunctional epoxy resin with satisfactory thermal, flame-retardant, and mechanical properties, Polym. Adv. Technol. 31 (1) (2020) 146–159.
[53] R.-K. Jian, Y.-F. Ai, L. Xia, L.-J. Zhao, H.-B. Zhao, Single component phosphamide-based intumescent flame retardant with potential reactivity towards low flammability and smoke epoxy resins, J. Hazard. Mater. 371 (2019) 529–539.
[54] Y.-Q. Shi, T. Fu, Y.-J. Xu, D.-F. Li, X.-L. Wang, Y.-Z. Wang, Novel phosphorus-containing halogen-free ionic liquid toward fire safety epoxy resin with well-balanced comprehensive performance, Chem. Eng. J. 354 (2018) 208–219.
[55] J. Luo, S. Yang, L. Lei, J. Zhao, Z. Tong, Toughening, synergistic fire retardation and water resistance of polydimethylsiloxane grafted graphene oxide to epoxy nanocomposites with trace phosphorus, Compos. Part A-Appl. Sci. Manuf. 100 (2017) 275–284.
[56] M. Chen, X. Lin, C. Liu, H. Zhang, An effective strategy to enhance the flame retardancy and mechanical properties of epoxy resin by using hyperbranched flame retardant, J. Mater. Sci. 56 (9) (2021) 5956–5974.
[57] N. Grassie, M.I. Guy, N.H. Tennent, Degradation of epoxy polymers: 2-Mechanism of thermal degradation of bisphenol-A diglycidyl ether, Polym. Degrad. Stabil. 13 (1) (1985) 11–20.
[58] Z.-M. Zhu, L.-X. Wang, L.-P. Dong, Influence of a novel P/N-containing oligomer on flame retardancy and thermal degradation of intumescent flame-retardant epoxy resin, Polym. Degrad. Stabil. 162 (2019) 129–137.
[59] K.A. Salmeia, S. Gaan, An overview of some recent advances in DOPO-derivatives: Chemistry and flame retardant applications, Polym. Degrad. Stabil. 113 (2015) 119–134.
[60] J. Zou, H. Duan, Y. Chen, S. Ji, J. Cao, H. Ma, A P/N/S-containing high-efficiency flame retardant endowing epoxy resin with excellent flame retardance, mechanical properties and heat resistance, Compos. Part B-Eng. 199 (2020), 108228.
[61] Z. Chi, Z. Guo, Z. Xu, M. Zhang, M. Li, L. Shang, Y. Ao, A DOPO-based phosphorus-nitrogen flame retardant bio-based epoxy resin from diphenolic acid: Synthesis, flame-retardant behavior and mechanism, Polym. Degrad. Stabil. 176 (2020) 109151, https://doi.org/10.1016/j.polymdegradstab.2020.109151.